

Multistage Entanglement Swapping

Alexander M. Goebel¹, Claudia Wagenknecht¹, Qiang Zhang², Yu-Ao Chen^{1,2}, Kai Chen^{2,*}, Jörg Schmiedmayer³, and Jian-Wei Pan^{1,2}

¹*Physikalisches Institut, Ruprecht-Karls-Universität Heidelberg, Philosophenweg 12, 69120 Heidelberg, Germany*

²*Hefei National Laboratory for Physical Sciences at Microscale and Department of Modern Physics, University of Science and Technology of China, Hefei, Anhui 230026, China*

³*Atominstitut der österreichischen Universitäten, TU-Wien, A-1020 Vienna, Austria*

(Dated: May 30, 2008)

We report an experimental demonstration of entanglement swapping over two quantum stages. By successful realizations of two cascaded photonic entanglement swapping processes, entanglement is generated and distributed between two photons, that originate from independent sources and do not share any common past. In the experiment we use three pairs of polarization entangled photons and conduct two Bell-state measurements (BSMs) one between the first and second pair, and one between the second and third pair. This results in projecting the remaining two outgoing photons from pair 1 and 3 into an entangled state, as characterized by an entanglement witness. The experiment represents an important step towards a full quantum repeater where multiple entanglement swapping is a key ingredient.

PACS numbers: 03.67.Bg, 03.67.Mn, 42.50.Dv, 42.50.Xa

Entanglement swapping is arguably one of the most important ingredients for quantum repeaters and quantum relays, which lays at the heart of quantum communication [1, 2, 3, 4]. For photonic quantum communication, the distance is largely limited due to decoherence from coupling to the environment and an increasing loss of photons in a quantum channel. This leads to an exponential decay in the fidelity of quantum information. This drawback can eventually be overcome by subdividing larger distances into smaller sections over which entanglement or quantum states can be distributed. The sections are then bridged by entanglement swapping processes [2, 3]. The swapping procedure therefore constitutes one of the key elements for a quantum relay [3], and a full quantum repeater [2] if combined with quantum purification [5, 6] and quantum memory [7]. As a result, quantum communication becomes feasible despite of realistic noise and imperfections. At the same time, the overhead for the used resources and communication time only increase polynomially with the distance [2, 3, 4].

Experimentally, photonic entanglement swapping has so far been successfully achieved for the case of discrete variables [8, 9], and for continuous variable [10], both via a single stage process. However, only after successful multiple swapping, will we be able to have a fully functional quantum repeater. There are additional advantages utilizing a multiple swapping process. For a quantum relay with many segments, it is equivalent to significantly lower the dark-count rate, which is a substantial factor limiting the transmission distance of successful quantum communication [3]. For quantum information carriers possessing mass, multiple swapping processes can speed up the distribution of entanglement by a factor that is proportional to the number of segments used [11]. Moreover, multistage entanglement swapping can improve the protection of quantum states against

noise from amplitude errors [11].

We report in this letter an experimental demonstration of a multiple entanglement swapping over two stages. This is achieved by utilizing three synchronous spatially independent pairs of polarization entangled photons, and performing BSMs among the three segments between the two communication parties. Two successful BSMs yield a final maximally entangled pair distributed between the two parties. To quantitatively evaluate the performance, we have observed the quality of the output state by the characterization of an entanglement witness, which confirms genuine entanglement generation. Our experiment implements an entanglement distribution over two distant stations which are initially independent of each other and have never physically interacted in the past. This proof-of-principle demonstration constitutes an important step towards robust long-distance quantum relays, quantum repeaters and related quantum protocols based on multiple entanglement swapping.

The principle for multistage entanglement swapping is sketched in Fig. 1. Consider three independent stations, each simultaneously emitting a pair of Einstein-Podolsky-Rosen (EPR) maximally entangled photons. In our experiments, we generate these states through the process of spontaneous parametric down-conversion [12]. By post-selecting events with only one photon in each output arm, we obtain polarization entangled photons in the state

$$|\Psi\rangle_{123456} = |\Psi^-\rangle_{12} \times |\Psi^-\rangle_{34} \times |\Psi^-\rangle_{56}, \quad (1)$$

where $|\Psi^-\rangle_{ij}$ is one of the four maximally entangled Bell states, which form a complete orthonormal basis for the joint state of two entangled photons

$$\begin{aligned} |\Psi^\pm\rangle_{ij} &= \frac{1}{\sqrt{2}}(|H\rangle_i|V\rangle_j \pm |V\rangle_i|H\rangle_j) \\ |\Phi^\pm\rangle_{ij} &= \frac{1}{\sqrt{2}}(|H\rangle_i|H\rangle_j \pm |V\rangle_i|V\rangle_j). \end{aligned}$$

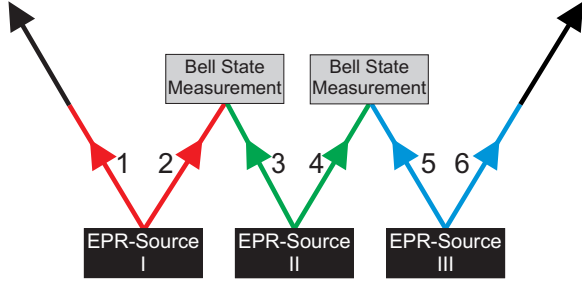


FIG. 1: Principle of multistage entanglement swapping: three EPR sources produce pairs of entangled photons 1-2, 3-4 and 5-6. Photon 2 from the initial state and photon 3 from the first ancillary pair are subjected to a joint BSM, and so are photon 4 from the first ancillary and photon 5 from the second ancillary pair. The two BSMs project outgoing photons 1 and 6 onto an entangled state. Thus the entanglement of the initial pair is swapped to an entanglement between photons 1 and 6.

Here $|H\rangle$ ($|V\rangle$) denotes the state of a horizontally (vertically) polarized photon. Note that photon pairs 1-2, 3-4 and 5-6 are entangled in an antisymmetric polarization state. The states of the three pairs are factorizable from each other, namely, there is no entanglement among photons from different pairs.

As a first step we perform a joint BSM on photons 2 and 3, that is, photons 2 and 3 are projected onto one of the four Bell states. This measurement also projects photons 1 and 4 onto a Bell state, in a form depending on the result of the BSM of photons 2 and 3. Close inspection shows that for the initial state given in Eq. (1), the emerging state of photons 1 and 4 is identical to the one that photons 2 and 3 collapse into. This is a consequence of the fact that the state of Eq. (1) can be rewritten as

$$\begin{aligned}
 |\Psi\rangle_{123456} = & \frac{1}{2} [|\Psi^+\rangle_{14}|\Psi^+\rangle_{23} - |\Psi^-\rangle_{14}|\Psi^-\rangle_{23} \\
 & - |\Phi^+\rangle_{14}|\Phi^+\rangle_{23} + |\Phi^-\rangle_{14}|\Phi^-\rangle_{23}] \\
 & \times |\Psi^-\rangle_{56}
 \end{aligned} \quad (2)$$

In all cases photons 1 and 4 emerge entangled despite the fact that they never interacted with one another in the past. The joint measurement of photons 2 and 3 tells about the type of entanglement between photons 1 and 4.

Without loss of generality, we assume in the first step that photons 2 and 3 have collapsed into the state $|\Phi^+\rangle_{23}$ as a result of the first BSM. The remaining four-photon state is then of the form

$$\begin{aligned}
 |\Psi\rangle_{1456} = & \frac{1}{2} [|\Psi^+\rangle_{16}|\Phi^-\rangle_{45} + |\Psi^-\rangle_{16}|\Phi^+\rangle_{45} \\
 & - |\Phi^+\rangle_{16}|\Psi^-\rangle_{45} - |\Phi^-\rangle_{16}|\Psi^+\rangle_{45}]
 \end{aligned} \quad (3)$$

In a similar manner we perform a second BSM on photons 4 and 5. Again a detection of the state $|\Phi^+\rangle_{45}$ results in projecting the remaining photons 1 and 6 onto the Bell

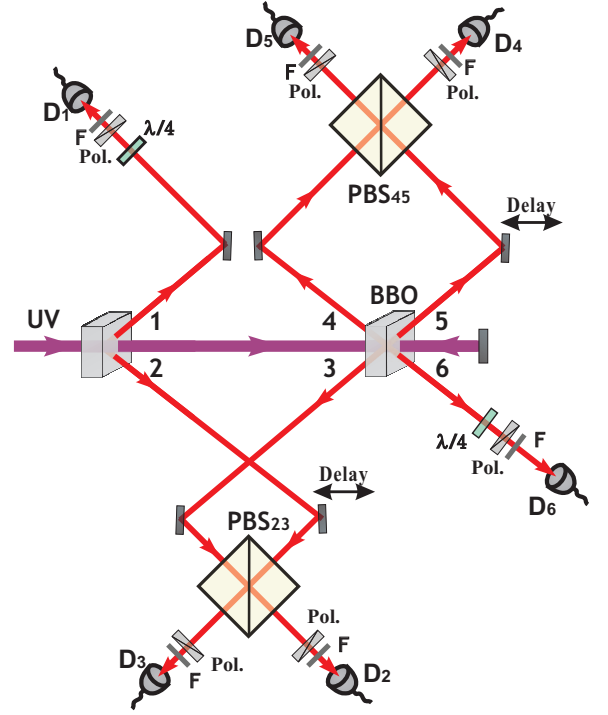


FIG. 2: The focused ultraviolet laser beam passes the first BBO generating photon pair 1-2. Refocused, it passes the second BBO generating the ancillary pair 5-6 and again retroreflected through the second BBO generating pair 3-4. In order to achieve indistinguishability at the interference PBS23 and PBS45 the spatial and temporal overlap are maximized by adjusting the delays and observing ‘Shih-Alley-Hong-Ou-Mandel’-type interference fringes [19] behind the PBS23 (PBS45) in the \pm basis [20]. With the help of polarizers and half/quarter wave plates, we are able to analyze the polarization of photons in arms 1 and 6. All photons are spectrally filtered by narrow band filters with $\Delta\lambda_{\text{FWHM}} \approx 2.8\text{nm}$ and are monitored by silicon avalanche single-photon detectors [21]. Coincidences are counted by a laser clocked field-programmable gate array based coincidence unit.

state

$$|\Psi^-\rangle_{16} = \frac{1}{\sqrt{2}}(|H\rangle_1|V\rangle_6 - |V\rangle_1|H\rangle_6) \quad (4)$$

A schematic diagram of our setup for multistage entanglement swapping is illustrated in Fig. 2. We use a pulsed high-intensity ultraviolet (UV) laser with a central wavelength of 390nm, a pulse duration of around 180 fs and a repetition rate of 76 MHz. The beam successively passes through two β -Barium-Borate (BBO) crystals, and is reflected to pass again through the second BBO to generate three polarization entangled photon pairs via type-II parametric down conversion [12].

Due to the high average power of 1W UV-light and improvements in collection efficiency and stability of the photon sources [13], we are able to observe up to 10^5 photon pairs per second from each source. With this bright-

ness of the entangled photon sources we could obtain around 4.5 six-photon events per minute in our setup.

For the joint BSM of photons 2 and 3 (photons 4 and 5), we choose to analyze the case of detecting the projection onto a $|\Phi^+\rangle$ state. Using a polarizing beam splitter (PBS) allows the projection of photons 2 and 3 (4 and 5) onto the state $|\Phi^+\rangle$ upon detecting a $|+\rangle|+\rangle$ or $|-\rangle|-\rangle$ coincidence at detectors D2 and D3 (D4 and D5) (with $|\pm\rangle = (|H\rangle \pm |V\rangle)/\sqrt{2}$). In our experiment only the $|+\rangle|+\rangle$ coincidences were registered, which reduces the overall success probability by a factor of 1/64. This could be improved by installing a half wave plate (HWP) at 22.5° , which corresponds to a polarization rotation of 45° , and a PBS after each output arm of PBS23 (PBS45). This configuration would also allow to detect the state $|\Phi^-\rangle$, which results in a $|+\rangle|-\rangle$ or $|-\rangle|+\rangle$ coincidence [14]. Thus, a factor of 1/4 for the overall success probability could be achieved in an ideal case.

As shown in equations Eq. (2,3,4) the projection measurements onto $|\Phi_{23}^+\rangle$ and $|\Phi_{45}^+\rangle$ leave photons 1 and 6 in the maximally entangled state $|\Psi_{16}^-\rangle$. In contrast to quantum state tomography, the measurement of witness operators does not provide a complete reconstruction of the original quantum state, it however allows to check with a minimal number of local measurements for an entanglement character of a quantum state. To verify that the two photons are really in an entangled state, and thus the swapping operation is successful, the expectation value of the corresponding witness operator [15, 16] is expected to take a negative value. In our case, the applied witness operator W is the most efficient one since it involves only the minimal number of local measurements [15]. It can be measured locally by choosing correlated measurement settings, that involve only the simultaneous detection of linear, diagonal and circular polarizations for both photons. We have performed local measurements on the outgoing state of photons 1 and 6 in the three complementary bases; linear (H/V), diagonal (+/-) and circular (R/L) (with $|L\rangle = (|H\rangle + i|V\rangle)/\sqrt{2}$ and $|R\rangle = (|H\rangle - i|V\rangle)/\sqrt{2}$).

The entanglement witness is given by

$$W = \frac{1}{2} (|HH\rangle\langle HH| + |VV\rangle\langle VV| + |++\rangle\langle ++| + |--\rangle\langle --| - |RL\rangle\langle RL| - |LR\rangle\langle LR|). \quad (5)$$

In the experiment, we perform measurements for each correlation function of the witness. The expectation values are shown in Fig. 3. Experimental integration time for each local measurement took about 60 hours and we recorded about 180 events of desired two-qubit coincidences. Every expectation value for a correlation function is obtained by making a von Neumann measurement along a specific basis and computing the probability over all the possible events. For example, for a HH correlation $\text{Tr}(\rho|HH\rangle\langle HH|)$, we perform measurements along the H/V basis. Then its value is given by the number of

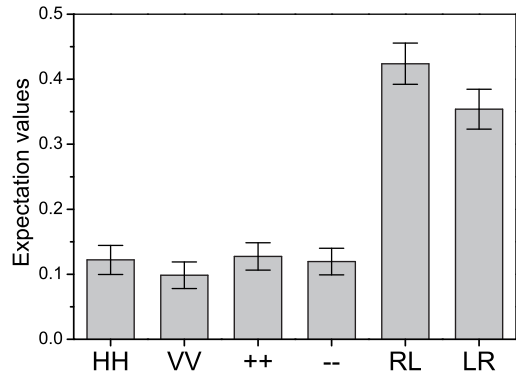


FIG. 3: Experimental expectation values for every correlation function of the entanglement witness for the swapped state. The results are derived by twofold coincidence measurements along three complementary common bases: a) $|H\rangle|V\rangle$; b) $|+\rangle|-\rangle$; and c) $|R\rangle|L\rangle$, conditioned on a fourfold coincidence event in $|++++\rangle$ for detectors D2-D3-D4-D5 which ensures two successful Bell state measurements.

coincidence counts of HH over the sum of all coincidence counts of HH, HV, VH and VV. We proceed likewise for the other correlation settings. The witness can then directly be evaluated to $\text{Tr}(\rho W) = -0.16 \pm 0.03$. The negativity of the measured witness implies clearly that entanglement has indeed been swapped. The imperfection of our data is due to the non-ideal quality of entangled states generated from the high power UV beam, as well as the partial distinguishability of independent photons at PBS23 and PBS45, which leads to non-perfect interferences and a degrading of entanglement output quality [17]. Moreover, double pair emission by a single source causes noise of an order of 10 spurious six-fold coincidences in 60 hours and was not subtracted in calculating the expectation value of the witness operator.

To ensure that there is no entanglement between photons 1 and 6 before either of the entanglement swapping process, we have performed a complete quantum state tomography. The experimental expectation values for various bases are illustrated in Fig. 4. Concurrence [18] is a monotonic function of entanglement, ranging from 0 for a separable state to 1 for a maximally entangled state. In terms of concurrence, we can thus quantify the degree of entanglement through a reconstructed density matrix ρ_{init} for the initial combined state from the data shown in Fig. 4. The concurrence C_{init} derived from ρ_{init} is $C_{init} = \max(0, -0.39 \pm 0.01) = 0$. As expected the concurrence is indeed 0, therefore photons 1 and 6 did not reveal any entanglement whatsoever before the swapping. Ideally, for a completely mixed state the expectation values for all local measurements should be 0,

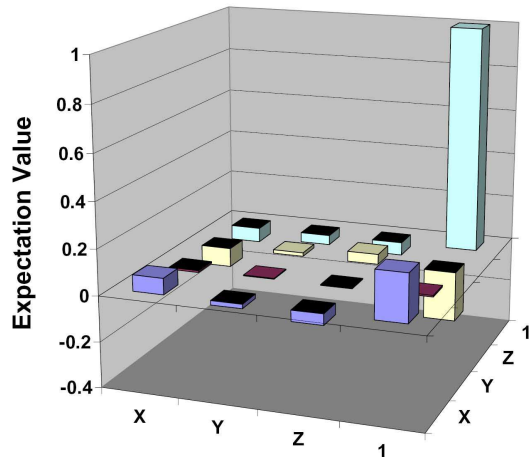


FIG. 4: Complete quantum state tomography on photon 1 and 6 before entanglement swapping. Label X corresponds to measurement setting σ_x , while Y and Z are for σ_y and σ_z , respectively. The result shows that the photons didn't reveal any entanglement whatsoever before the swapping operation.

except for the unity operator, which should be 1. The contributions of the measurement settings other than the unity operator are mainly due to noise caused by scattered light of the UV beam at the BBO crystal. For convenience of comparison, we also performed the same witness measurement of Eq. (5) to give $\langle W \rangle = 0.28 \pm 0.01$, which is safely above the bound $\langle W \rangle < 0$ needed to reveal entanglement. However, after the two-stage entanglement swapping, entanglement arises as unambiguously confirmed by negativity of expectation value for the witness $\langle W \rangle = -0.16 \pm 0.03$ as discussed above.

In conclusion, we have for the first time provided a proof-of-principle demonstration of a two-stage entanglement swapping using photonic qubits. The feasibility and effectiveness of this process has been verified by a successful distribution of genuine entanglement after two simultaneously independent swapping process. This result yields the possibility of immediate near-future applications of various practical quantum information processing tasks. If combined with narrow-band entanglement sources, the implementation of quantum relays (without quantum memory) and quantum repeaters (with quantum memory) would become within current reach [2, 7, 9], as well as quantum state transfer and quantum cryptography networks in a more efficient way and over much larger distances of around hundreds of kilometers [3]. Our demonstration also allows for the possibility of utilizing multi-party, multiple stages entanglement swapping to achieve global quantum communication networks though with significant challenges ahead [11].

This work was supported by the Marie Curie Excel-

lence Grant from the EU, the Alexander von Humboldt Foundation, the National Fundamental Research Program of China under Grant No.2006CB921900, the CAS, and the NNSFC. K.C acknowledges support of the Bairen program of CAS. C.W. was additionally supported by the Schlieben-Lange Program of the ESF.

* Electronic address: kaichen@ustc.edu.cn

- [1] M. Zukowski, A. Zeilinger, M.A. Horne, and A.K. Ekert, *Phys. Rev. Lett.* **71**, 4287 (1993).
- [2] H.J. Briegel, W. Dur, J.I. Cirac, and P. Zoller, *Phys. Rev. Lett.* **81**, 5932 (1998); W. Dur, H.J. Briegel, J.I. Cirac, and P. Zoller, *Phys. Rev. A* **59**, 169 (1999).
- [3] E. Waks, A. Zeevi, and Y. Yamamoto, *Phys. Rev. A* **65**, 052310 (2002); B.C. Jacobs, T.B. Pittman, and J.D. Franson, *ibid.* **66**, 052307 (2002); D. Collins, N. Gisin, H.D. Riedmatten, *J. Mod. Opt.* **52**, 735 (2005).
- [4] P. Zoller, J.I. Cirac, L.M. Duan and J.J. Garcia-Ripoll, in "Quantum entanglement and information processing", Proceedings of the Les Houches Summer School, Session 79, edited by D. Estève, J.M. Raimond and J. Dalibard (Elsevier, Amsterdam, 2004).
- [5] C.H. Bennett, D.P. DiVincenzo, J.A. Smolin, and W.K. Wootters, *Phys. Rev. A* **54**, 3824 (1996).
- [6] P.G. Kwiat, S. Barraza-Lopez, A. Stefanov, and N. Gisin, *Nature (London)* **409**, 1014 (2001). J.-W. Pan, C. Simon, Č. Brukner, and A. Zeilinger, *Nature (London)* **410**, 1067 (2001); J.-W. Pan, S. Gasparoni, R. Ursin, G. Weihs, and A. Zeilinger, *Nature (London)* **423**, 417 (2003).
- [7] T. Chanelière *et al.*, *Nature (London)* **438**, 833 (2005); D. Felinto *et al.*, *Nature Phys.* **2**, 844 (2006); Y.A. Chen *et al.*, *Nature Phys.* **4**, 103 (2008).
- [8] J.-W. Pan, D. Bouwmeester, H. Weinfurter, and A. Zeilinger, *Phys. Rev. Lett.* **80**, 3891 (1998); T. Jennewein, G. Weihs, J.-W. Pan, and A. Zeilinger, *ibid.* **88**, 017903 (2001); H. de Riedmatten *et al.*, *Phys. Rev. A* **71**, 050302(R) (2005).
- [9] M. Halder, *et al.*, *Nature Phys.* **3**, 692 (2007).
- [10] R.E.S. Polkinghorne, and T. C. Ralph, *Phys. Rev. Lett.* **83**, 2095 (1999); X.J. Jia *et al.*, *ibid.* **93**, 250503 (2004); N. Takei, H. Yonezawa, T. Aoki, and A. Furusawa, *ibid.* **94**, 220502 (2005).
- [11] S. Bose, V. Vedral, and P.L. Knight, *Phys. Rev. A* **57**, 822 (1998).
- [12] P.G. Kwiat *et al.*, *Phys. Rev. Lett.* **75**, 4337 (1995).
- [13] Q. Zhang *et al.*, *Nature Phys.* **2**, 678 (2006).
- [14] J.-W. Pan and A. Zeilinger, *Phys. Rev. A* **57**, 2208-2211 (1998).
- [15] O. Gühne *et al.*, *Phys. Rev. A* **66**, 062305 (2002).
- [16] M. Barbieri *et al.*, *Phys. Rev. Lett.* **91**, 227901 (2003).
- [17] V. Scarani *et al.*, *Eur. Phys. J. D* **32**, 129 (2005); M. Barbieri, *Phys. Rev. A* **76**, 043825 (2007).
- [18] W.K. Wootters, *Phys. Rev. Lett.* **80**, 2245 (1998).
- [19] Y.H. Shih and C.O. Alley, *Phys. Rev. Lett.* **61**, 2921 (1988); C.K. Hong, Z.Y. Ou, and L. Mandel, *ibid.* **59**, 2044 (1987).
- [20] J.-W. Pan, M. Daniell, S. Gasparoni, G. Weihs, and A. Zeilinger, *Phys. Rev. Lett.* **86**, 4435 (2001).
- [21] M. Zukowski, A. Zeilinger, and H. Weinfurter, *Ann. NY Acad. Sci.* **755**, 91 (1995).